



HAL
open science

Subproblem Approach for Thin Shell Dual Finite Element Formulations

Vuong Quoc Dang, Patrick Dular, Ruth V. Sabariego, Laurent Krähenbühl,
Christophe Geuzaine

► **To cite this version:**

Vuong Quoc Dang, Patrick Dular, Ruth V. Sabariego, Laurent Krähenbühl, Christophe Geuzaine. Subproblem Approach for Thin Shell Dual Finite Element Formulations. *Compumag 2011*, Jul 2011, Sydney, Australia. pp.électronique. hal-00578978

HAL Id: hal-00578978

<https://hal.science/hal-00578978>

Submitted on 22 Mar 2011

HAL is a multi-disciplinary open access archive for the deposit and dissemination of scientific research documents, whether they are published or not. The documents may come from teaching and research institutions in France or abroad, or from public or private research centers.

L'archive ouverte pluridisciplinaire **HAL**, est destinée au dépôt et à la diffusion de documents scientifiques de niveau recherche, publiés ou non, émanant des établissements d'enseignement et de recherche français ou étrangers, des laboratoires publics ou privés.

Subproblem Approach for Thin Shell Dual Finite Element Formulations

Vuong Q. Dang¹, Patrick Dular^{1,2}, Ruth V. Sabariego¹, Laurent Krähenbühl³ and Christophe Geuzaine¹

¹Dept. of Electrical Engineering and Computer Science, University of Liège, Belgium, Vuong.DangQuoc@student.ulg.ac.be

²Fonds de la Recherche Scientifique - F.R.S.-FNRS, Belgium

³Université de Lyon, Ampère (CNRS UMR5005), École Centrale de Lyon, F-69134 Écully Cedex, France

Abstract—A subproblem technique is applied on dual formulations to the solution of thin shell finite element models. Both the magnetic vector potential and magnetic field formulations are considered. The subproblem approach developed herein couples three problems: a simplified model with inductors alone, a thin region problem using approximate interface conditions, and a correction problem to improve the accuracy of the thin shell approximation, in particular near their edges and corners. Each problem is solved on its own independently defined geometry and finite element mesh.

I. INTRODUCTION

The solution by means of subproblems provides clear advantages in repetitive analyses and can also help in improving the overall accuracy of the solution [1], [2]. In the case of thin shell (TS) problems the method allows to benefit from previous computations instead of starting a new complete finite element (FE) solution for any variation of geometrical or physical characteristics. Furthermore, It allows separate meshes for each subproblem, which increases computational efficiency.

In this paper, a problem ($p = 1$) involving massive or stranded inductors alone is first solved on a simplified mesh without thin regions. Its solution gives surface sources (SSs) for a TS problem ($p = 2$) through interface conditions (ICs), based on a 1-D approximation [3], [4]. The TS solution is then considered as a volume source (VSs) of a correction problem ($p = 3$) taking the actual field distribution of the field near edges and corners into account, which are poorly represented by the TS approximation. The method is validated on a practical test problem using a classical *brute force* volume formulation.

II. DEFINITION OF THE SUBPROBLEM APPROACH

A. Canonical magnetodynamic or static problem

A canonical magnetodynamic or static problem p , to be solved at step p of the subproblem approach, is defined in a domain Ω , with boundary $\partial\Omega_p = \Gamma_p = \Gamma_{h,p} \cup \Gamma_{b,p}$. Subscript p refers to the associated problem p . The equations, material relations and boundary conditions (BCs) of the subproblems ($p = 1, 2, 3$) are:

$$\text{curl } \mathbf{h}_p = \mathbf{j}_p, \quad \text{div } \mathbf{b}_p = 0, \quad \text{curl } \mathbf{e}_p = -\partial_t \mathbf{b}_p, \quad (1)$$

$$\mathbf{h}_p = \mu_p^{-1} \mathbf{b}_p + \mathbf{h}_{s,p}, \quad \mathbf{j}_p = \sigma_p \mathbf{e}_p + \mathbf{j}_{s,p}, \quad (2)$$

$$\mathbf{n} \times \mathbf{h}_p|_{\Gamma_{h,p}} = \mathbf{j}_{su,p}, \quad \mathbf{n} \cdot \mathbf{b}_p|_{\Gamma_{b,p}} = \mathbf{b}_{su,p}, \quad (3)$$

$$\mathbf{n} \times \mathbf{e}_p|_{\Gamma_{e,p} \subset \Gamma_{b,p}} = \mathbf{k}_{su,p}, \quad (4)$$

where \mathbf{h}_p is the magnetic field, \mathbf{b}_p is the magnetic flux density, \mathbf{e}_p is the electric field, $\mathbf{j}_{s,p}$ is the electric current density, μ_p is the magnetic permeability, σ_p is the electric conductivity

This work has been supported by the Belgian Science Policy (IAP P6/21) and the Belgian French Community (ARC 09/14-02).

and \mathbf{n} is the unit normal exterior to Ω_p . In what follows the notation $[\cdot]_{\gamma_p} = \cdot|_{\gamma_p^+} - \cdot|_{\gamma_p^-}$ expresses the discontinuity of a quantity through any interface γ_p (with sides γ_p^+ and γ_p^-) in Ω_p , defining interface conditions (ICs).

The fields $\mathbf{h}_{s,p}$ and $\mathbf{j}_{s,p}$ in (2) are VSs in the subproblem approach which can be used for expressing changes of permeability or conductivity (via $\mathbf{h}_{s,p}$ and $\mathbf{j}_{s,p}$, respectively). Indeed, changing from μ_1 and σ_1 in a given subregion for problem $p = 1$ to μ_2 and σ_2 for problem $p = 2$ leads to the associated VSs

$$\mathbf{h}_{s,2} = (\mu_2^{-1} - \mu_1^{-1}) \mathbf{b}_1, \quad \mathbf{j}_{s,2} = (\sigma_2 - \sigma_1) \mathbf{e}_1. \quad (5)$$

B. Constraints between subproblems

The constraints for the problems ($p = 2, 3$) are respectively SSs and VSs. The TS model ($p = 2$) [4] is written as a subproblem following the inductor source field calculation of problem ($p = 1$). Its SSs are defined via ICs of impedance-type boundary conditions (IBC) combined with contributions from problem ($p = 1$). The \mathbf{b} -formulation uses a magnetic vector potential $\mathbf{a} = \mathbf{a}_c + \mathbf{a}_d$ (such that $\text{curl } \mathbf{a} = \mathbf{b}$). The \mathbf{h} -formulation uses a similar decomposition, $\mathbf{h} = \mathbf{h}_c + \mathbf{h}_d$. Fields \mathbf{a}_c , \mathbf{h}_c and \mathbf{a}_d , \mathbf{h}_d are respectively continuous and discontinuous through the TS. The weak \mathbf{b} - and \mathbf{h} -formulations involve the SSs in surface integral terms, respectively

$$\langle [\mathbf{n} \times \mathbf{h}_2]_{\gamma_2}, \mathbf{a}'_c + \mathbf{a}'_d \rangle_{\gamma_2}, \quad \langle [\mathbf{n} \times \mathbf{e}_2]_{\gamma_2}, \mathbf{h}'_c + \mathbf{h}'_d \rangle_{\gamma_2} \quad (6a-b)$$

with \mathbf{a}_d and \mathbf{h}_d defined as equal to zero on the side γ_2^- of the shell and $\gamma = \gamma_1^\pm = \gamma_2^\pm$; \mathbf{a}'_d , \mathbf{h}'_d , \mathbf{a}'_c and \mathbf{h}'_c are test functions. To explicitly express the field discontinuities, (6a-b) are rewritten as

$$\langle [\mathbf{n} \times \mathbf{h}_2]_{\gamma_2}, \mathbf{a}'_c \rangle_{\gamma_2} + \langle \mathbf{n} \times \mathbf{h}_2, \mathbf{a}'_d \rangle_{\gamma_2^+}, \quad (7)$$

$$\langle [\mathbf{n} \times \mathbf{e}_2]_{\gamma_2}, \mathbf{h}'_c \rangle_{\gamma_2} + \langle \mathbf{n} \times \mathbf{e}_2, \mathbf{h}'_d \rangle_{\gamma_2^+}. \quad (8)$$

The involved tangential fields in (7) and (8) are given by the TS model but some have to be corrected. The discontinuities in the first terms do not need any correction because solution ($p = 1$) presents no such discontinuities, i.e. $[\mathbf{n} \times \mathbf{h}_1]_{\gamma_1} = 0$ and $[\mathbf{n} \times \mathbf{e}_1]_{\gamma_1} = 0$. The tangential fields in the second terms have to be corrected with the opposite tangential contributions from solution ($p = 1$), i.e. $-\mathbf{n} \times \mathbf{h}_1|_{\gamma_2}$ and $-\mathbf{n} \times \mathbf{e}_1|_{\gamma_2}$. The resulting surface integral terms are correctly expressed via the weak formulations of problem ($p = 1$), thus rather via volume integrals, i.e.

$$\langle \mathbf{n} \times \mathbf{h}_1, \mathbf{a}'_d \rangle_{\gamma_2^+} = -(\mu_1^{-1} \text{curl } \mathbf{a}_1, \text{curl } \mathbf{a}'_d)_{\Lambda_1^+} - (\sigma_1 \partial_t \mathbf{a}_1, \mathbf{a}'_d)_{\Lambda_1^+} \quad (9)$$

$$\langle \mathbf{n} \times \mathbf{e}_1, \mathbf{h}'_d \rangle_{\gamma_2^+} = -(\mu_1^{-1} \partial_t \mathbf{h}_s, \mathbf{h}'_d)_{\Lambda_1^+} - (\mu_1^{-1} \partial_t \mathbf{h}_1, \mathbf{h}'_d)_{\Lambda_1^+} \quad (10)$$

with the volume integrals limited to a single layer of FEs Λ_1^+ touching $\gamma_2^+ = \gamma_1^+$, because they involve only the traces $\mathbf{n} \times \mathbf{a}'_d|_{\gamma_2^+}$ and $\mathbf{n} \times \mathbf{h}'_d|_{\gamma_2^+}$. Once obtained, the TS solution ($p =$

2) is then corrected by problem ($p = 3$) that overcomes the TS assumptions [4]. It has to suppress the TS representation, via VSs in the added volumic shell that account for the volumic change of μ_p and σ_p in problem ($p = 3$) that characterized the ambient region (using (5) with $\mu_2 = \mu_0$, $\mu_3 = \mu_{volume}$, $\sigma_2 = 0$ and $\sigma_3 = \sigma_{volume}$). This correction will be shown to be limited to the neighborhood of the shell, which allows to benefit from a reduction of the extension of the associated mesh.

III. APPLICATION EXAMPLE

The test problem is a shielded induction heater. It comprises two inductors (stranded or massive), a plate ($\mu_{r,plate} = 100$, $\sigma_{plate} = 1 \text{ MS/m}$) in the middle, and two screens ($\mu_{r,screen} = 1$, $\sigma_{screen} = 37.7 \text{ MS/m}$) (Fig. 1). It is first considered via a stranded inductor model (Fig. 2, top left, a_1), adding a TS FE model (Fig. 2, bottom left, a_2) that does not include the inductor anymore. Finally, a correction problem replaces the TS FEs with classical volume FEs (Fig. 2, top right, a_3). The complete solution is shown as well (Fig. 2, bottom right, $a_1 + a_2 + a_3$). Errors on the magnetic flux with the TS model between classical solution and ($p = 1 + 2$) for both b - and h -formulations are shown in (Fig. 3); they can nearly reach 65% in the end regions of the plate. Accurate local corrections can then be obtained, reducing the errors to less than 0.01% (Fig. 4). Significant TS errors are achieved for the eddy current as well (Fig. 5), up to 50% and 60% near the screen ends for ($\delta = 0.918 \text{ mm}$, $\mu_{r,plate} = 100$, $f = 3 \text{ kHz}$) and ($\delta = 0.65 \text{ mm}$, $\mu_{r,plate} = 200$, $f = 3 \text{ kHz}$) respectively, with $d = 4 \text{ mm}$ and $\sigma_{plate} = 1 \text{ MS/m}$ in both cases. The proposed technique for TS FE and correction have been presented via a subproblem approach. It leads to accurate eddy current and magnetic flux distributions at the edges and corners of thin regions. All the steps of the method will be detailed, illustrated and validated in extended paper for both b - and h - formulations in 2D and 3D cases.

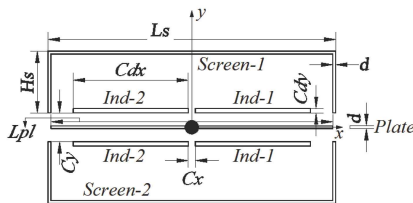


Fig. 1. Shielded induction heater ($L_{pl} = 2.2 \text{ m}$, $L_s = 2 \text{ m}$, $H_s = 400 \text{ mm}$, $C_{dz} = 800 \text{ mm}$, $C_{dx} = 10 \text{ mm}$, $C_y = 200 \text{ mm}$, $C_z = 50 \text{ mm}$, $d = 5 \text{ mm}$)

REFERENCES

- [1] P. Dular, Vuong Q. Dang, R. V. Sabariego, L. Krähenbühl and C. Geuzaine, "Correction of thin shell finite element magnetic models via a subproblem method," IEEE Trans. Magn., accepted for publication.
- [2] P. Dular, R. V. Sabariego, C. Geuzaine, M. V. Ferreira da Luz, P. Kuo-Peng and L. Krähenbühl, "Finite Element Magnetic Models via a Coupling of Subproblems of Lower Dimensions," IEEE Trans. Magn., vol. 46, no. 8, pp. 2827–2830, 2010.
- [3] L. Krähenbühl and D. Müller, "Thin layers in electrical engineering. Examples of shell models in analyzing eddy-currents by boundary and finite element methods," IEEE Trans. Magn., vol. 29, no. 2, pp. 1450–1455, 1993.
- [4] C. Geuzaine, P. Dular, and W. Legros, "Dual formulations for the modeling of thin electromagnetic shells using edge elements," IEEE Trans. Magn., vol. 36, no. 4, pp. 799–802, 2000.

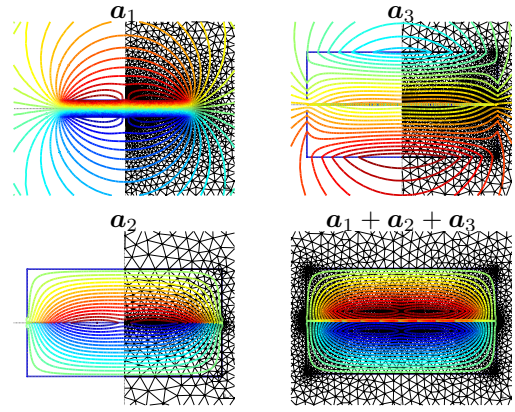


Fig. 2. Flux lines (real part) for the total solution ($a_1 + a_2 + a_3$), the stranded inductor model (a_1), thin shell added (a_2) and volume solution (a_3) with the different meshes used ($d = 4 \text{ mm}$, $f = 1 \text{ kHz}$)

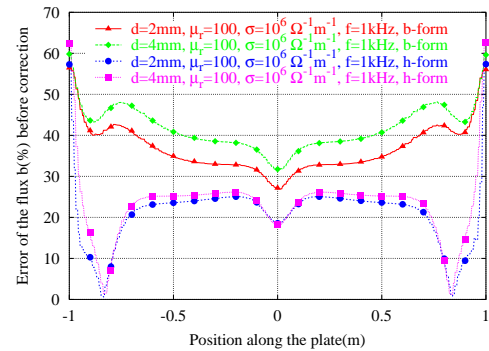


Fig. 3. Errors on the magnetic flux before correction along the plate with different thicknesses and effects of μ_r , σ and frequency f

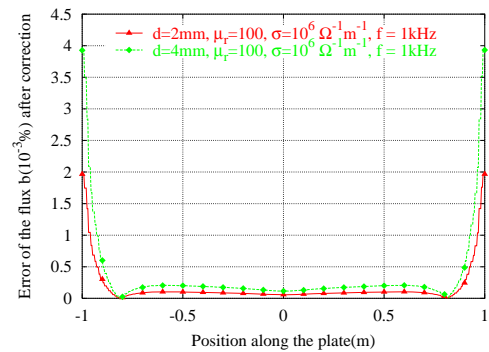


Fig. 4. Errors on the magnetic flux along the plate after correction with different thicknesses and effects of μ_r , σ and frequency f

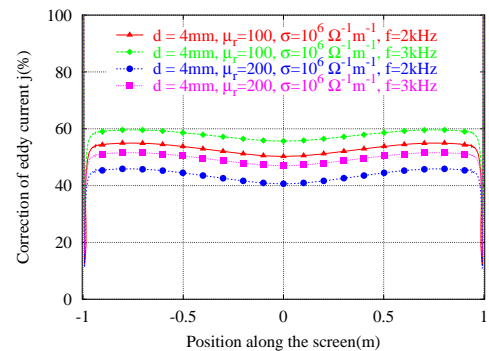


Fig. 5. Errors on the eddy current along the screen for b - formulation with effects of μ_r , σ and frequency f